Eur J Med Chem (1997) 32, 669–675

Laboratory note

Addition of Tyr at the N-terminal to bradykinin preserves its overall conformation*

S Srivastava[1]**, RS Phadke[1], SA Kamath[2], EC Coutinho[2]

[1]*Tata Institute of Fundamental Research, Homi Bhabha Road, Colaba, Mumbai 400005;*
[2]*Bombay College of Pharmacy, Kalina, Santacruz (E), Mumbai 400 098, India*

(Received 9 October 1996; accepted 6 February 1997)

Summary — Bradykinin, Arg–Pro–Pro–Gly–Phe–Ser–Pro–Phe–Arg (BK), possesses diverse pharmacological activity. Addition of Tyr to the N-terminal of BK (Tyr-BK) retains 90% of the activity. The conformation of Tyr-BK has been investigated by 2D-NMR. Two important conformations have been detected in solution. In the first conformation X the amide bond between Ser^7–Pro^8 is *cis*. The second conformation Y has both the Pro^3–Pro^4 and Ser^7–Pro^8 amide bonds as *cis*. In conformation X, β-turns are found around the segments P3–P4–G5–F6 and S7–P8–F9–R10. A total of 20 distance restraints based on observed nOes have been used in a molecular dynamics (MD) simulation to generate the solution structures. The slightly lower activity of Tyr-BK has been explained based on structural similarities and differences with native BK.

Tyr-bradykinin / conformation / NMR structure / molecular dynamics

Introduction

Bradykinin, Arg–Pro–Pro–Gly–Phe–Ser–Pro–Phe–Arg (BK), is a peptide hormone which has been implicated in various pathological conditions in man [1]. It is known to possess potent vasodilatory and algesic activity [2]. Contractile activity in smooth muscle preparations has been observed in response to BK.

Modifications to BK have been made in an attempt to understand the structural requirements for biological activity. Understanding changes in the conformation due to modifications in the structure with resulting loss or enhancement of activity will help in the design of more potent analogs [3–5]. Native BK and its analogs were studied earlier by ourselves and others [3, 6–10]. Alteration of amino acids at both the N- and C-termini has a profound effect on activity. Thus des[Arg^1]-BK and des[Arg^9]-BK are devoid of activity [11]. Replacement of Arg^1 by Lys retains only 10% of the activity [12]. The peptide [$Tyr]^8$-BK has been synthesised by replacing Phe at the 8 position of native BK with Tyr, with a view to radiolabelling the peptide (^{125}I-labelled). The radiolabelled peptide is convenient for assays in medical diagnosis. It has been used in the investigation of the action of kinins on the kidney under both physiological and pathological conditions [13]. Unfortunately, it has been found that this analog is much less potent than the native peptide [14]. Our earlier NMR studies on this peptide indicate that the peptide loses conformational rigidity on replacing Phe^8 by Tyr [7]. However, addition of Tyr at the N-terminal, ie, Tyr–Arg–Pro–Pro–Gly–Phe–Ser–Pro–Phe–Arg (Tyr-BK) was found to retain 90% of the activity of native BK in vitro tests on rat and bovine uterus [15] and is thus a better candidate for radiolabelling assay.

With this in view, we investigated the effect of the addition of Tyr on the conformation of BK and report here the results of our findings. We have made an attempt to correlate the conformation with the slightly lower activity of Tyr-BK.

NMR

Methodology

Tyr-BK was purchased from Sigma Chemical Co, USA. For NMR experiments the peptide was dissolved in DMSO–d_6. NMR experiments were carried

*This paper was presented at ICMRBS held at Keystone, CO, USA, August 18–23, 1996.
**Correspondence and reprints.

out on a Bruker AMX-500 FT NMR spectrometer. Resonance assignments were made using 2D-COSY [16] and NOESY [17] with conventional pulse sequences and a relaxation delay of 1 s. The conformation of the molecule was inferred from NOESY spectra recorded with mixing times varying from 300–500 ms, chemical shifts, temperature coefficients of NH chemical shifts measured in the temperature range 298–325 K and $^3J_{NH\alpha}$ coupling constants. The chemical shifts were reported with respect to the residual DMSO peak at 2.5 ppm.

NMR results

The 1D-spectrum of Tyr-BK is shown in figure 1a, and the COSY spectrum in figure 1b. In the fingerprint region of the COSY spectrum (fig 1c) seven cross-peaks are observed. The three prolines having no NH protons do not exhibit NH–Cα connectivity. The resonances of the individual amino acids were identified in the COSY spectrum based on their spin systems. Ser (S7), Phe (F6 and F9) and Tyr (Y1) all have an AMX spin system. However, the β-protons of Ser occur more downfield than Phe and Tyr and help to distinguish Ser. Gly (G5) could be easily identified from its unique spin system, the two α-protons showing up as separate resonances and exhibiting individual coupling to the NH resonance. Pro (P3, P4 and P8) has a spin system $A_2(T_2)MPX$ which is similar to Arg (R2 and R10). However, the arginines (R2 and R10) could be identified from their ε–NH resonances downfield at ca 8.73 and 8.92 ppm respectively which are coupled to their CδH protons in the COSY spectrum. Using this as a starting point, we traced back the connectivity to the CαH protons. Having identified and grouped the amino acids based on their spin systems, the NOESY spectrum (fig 2a) was used for the sequential assignments [18].

Sequential assignments

Starting with the COSY cross-peak of S7, a vertical line meets the NOESY peak to F6. A horizontal line to the left meets the COSY peak of F6. Again, on moving up we find two NOESY peaks to the two αHs of G5. Continuing in this fashion, by alternately locating COSY and NOESY peaks, unique resonance assignments are made up to P4. A break in the assignment occurs due to absence of an NH resonance in P4. The NOESY peaks from P4δH to P3αH and from P3δH to R2αH help in assigning P3 and R2. No NOESY peak is seen between R2NH and Y1αH. On the C-terminal side, the triad P8–F9–R10 was sequentially identified using the same strategy as that for identifying COSY and NOESY peaks as described

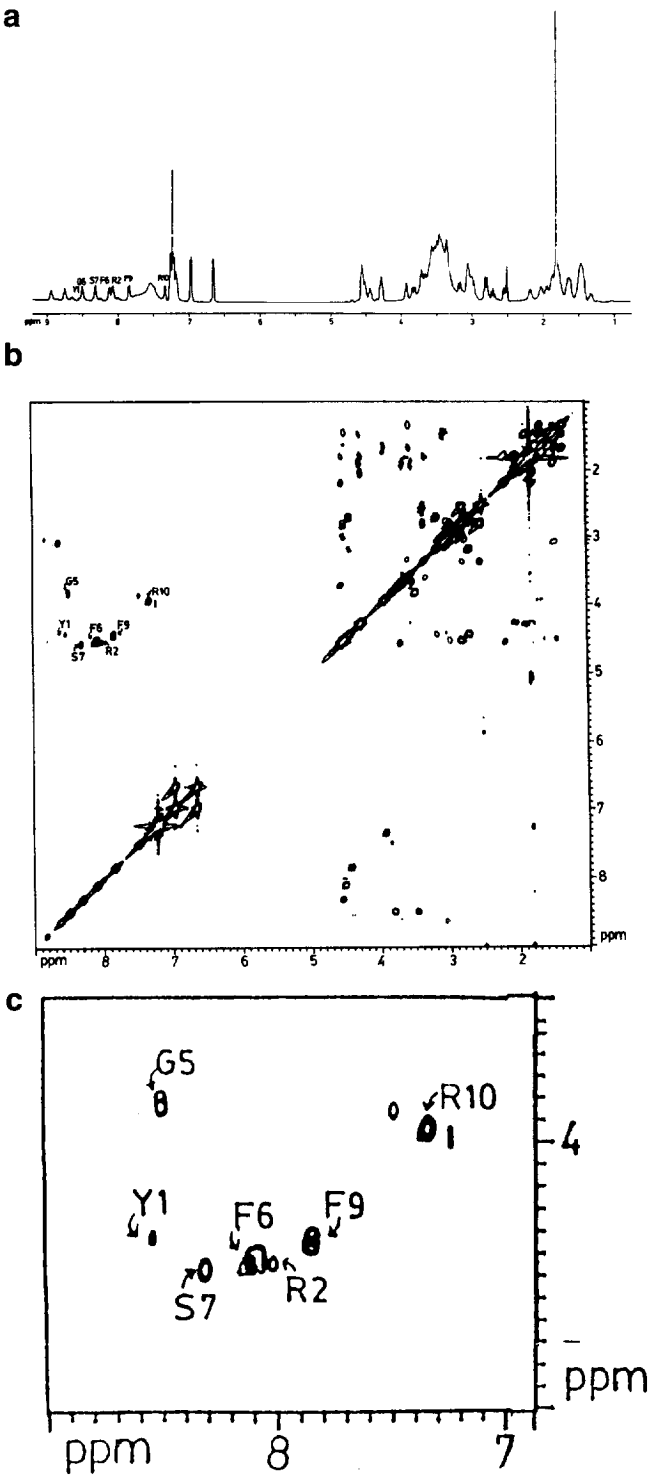

Fig 1. a. 500 MHz ^{1}H-NMR; **b.** COSY spectrum of Tyr-BK in DMSO–d_6 at 298 K; **c.** Expansion of fingerprint region of the COSY spectrum.

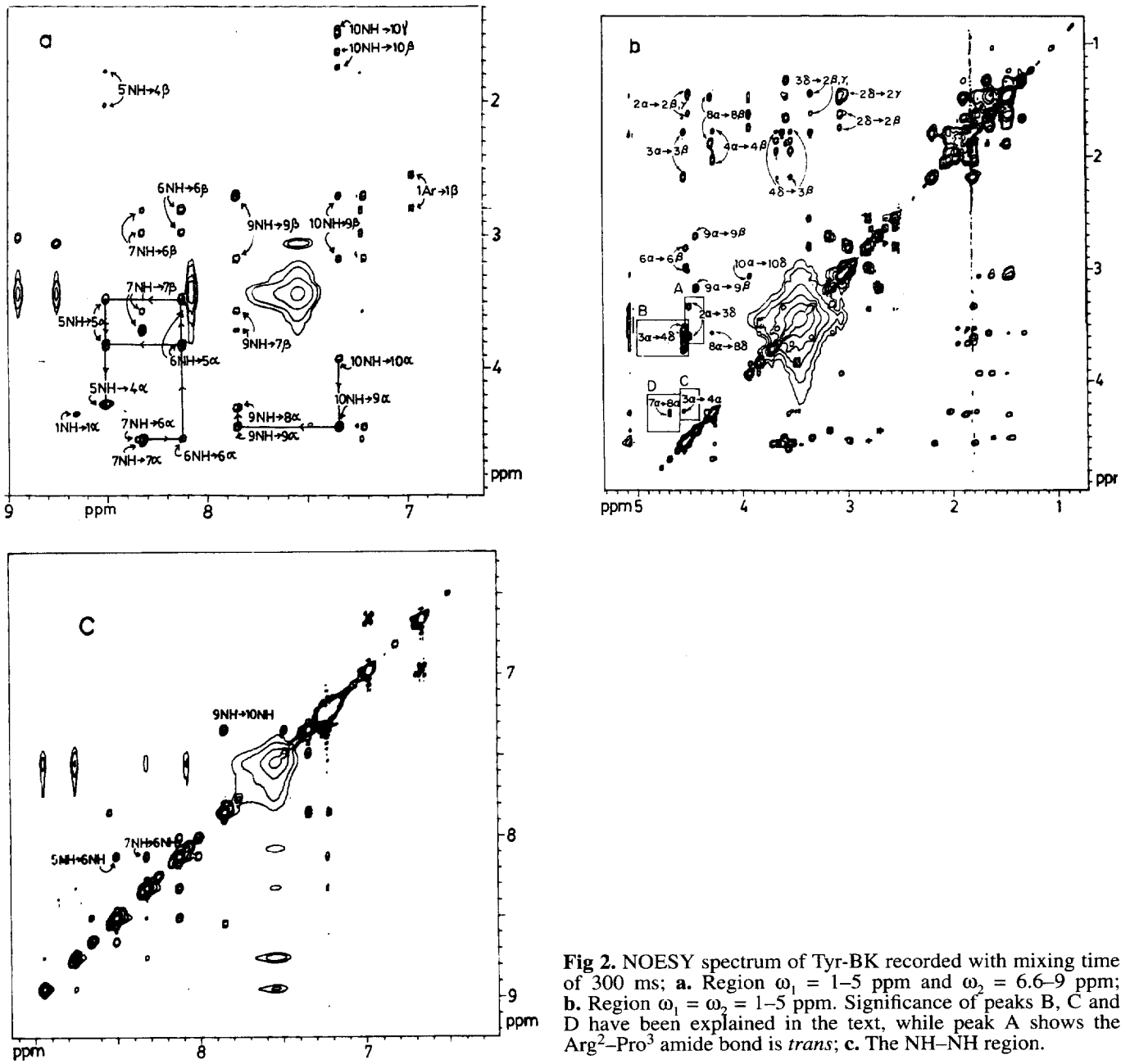

Fig 2. NOESY spectrum of Tyr-BK recorded with mixing time of 300 ms; **a.** Region ω_1 = 1–5 ppm and ω_2 = 6.6–9 ppm; **b.** Region $\omega_1 = \omega_2$ = 1–5 ppm. Significance of peaks B, C and D have been explained in the text, while peak A shows the Arg^2–Pro^3 amide bond is *trans*; **c.** The NH–NH region.

above. The only unassigned peak in the finger print region was labelled Y1. The COSY peak between CαH and CβH of Tyr was not seen and may be due to some specific conformation around the Cα–Cβ bond which makes the coupling constant too small to be observed. However, the βHs of Y1 were identified from NOESY peaks with the ortho protons on the ring. This completes the assignment of the entire peptide. The chemical shifts are shown in table I.

As discussed below there are two conformations of Tyr-BK, labelled X (dominant) and Y (minor). The assignments given above are only for the dominant conformation X. The few peaks from the minor conformation Y observed in the NH region are difficult to assign since no connectivity can be traced to a separate set of peaks in the upfield region. This situation could be due to an overlap of the peaks belonging to the major and minor conformations.

Table I. Chemical shifts (ppm) of protons of Tyr-BK in DMSO–d_6 at 298 K.

Residue	*NH*	*CαH*	*CβH*	*Others*
Tyr1	–	–	2.55, 2.80	6.65, 6.97 (aromatic)
Arg2	8.08	4.47	1.60, 1.75	1.45 (CγH, CδH) 2.96 (CεH), 8.73 (εNH_2)
Pro3	–	4.52	1.77, 2.19	3.32, 3.58 (CδH)
Pro4	–	4.22	1.77, 2.01	3.52, 3.69 (CδH)
Gly5	8.50	3.48, 3.82	–	–
Phe6	8.12	4.50	2.78, 2.96	7.16–7.25 (aromatics)
Ser7	8.32	4.55	3.57, 3.70	–
Pro8	–	4.27	1.48, 1.86	3.52, 3.69 (CδH)
Phe9	7.84	4.43	2.70, 3.19	7.16–7.25 (aromatics)
Arg10	7.35	3.95	1.60, 1.75	1.45 (CγH, CδH) 3.06 (CδH), 8.92 (εNH_2)

Conformation

The conformation of the peptide has been deduced from the NMR parameters: chemical shifts (differences from random coil values), $^3J_{NH\alpha}$ coupling constants, temperature coefficients of NH chemical shifts and nuclear Overhauser effects [19]. For a small peptide like the one studied here, the molecule is expected to exhibit high dynamics and NMR will reveal only an average conformation.

The $^3J_{NH\alpha}$ coupling constants are listed in table II. The $^3J_{NH\alpha}$ coupling constant is related to the dihedral angle ϕ by the Karplus relationship [20]. However, ϕ is not uniquely determined and must be deduced in conjunction with other NMR data.

Changes in the NH chemical shift with temperature ($-\Delta\delta/\Delta T$) provide clues to their involvement in intramolecular H-bonding or solvent shielding [21]. Values < 0.003 ppm K^{-1} are indicative of H-bonding or solvent shielding, while values > 0.005 ppm K^{-1} show exposure to the solvent. No firm conclusion can be made in the range 0.003–0.005 ppm K^{-1}. The temperature coefficients are given in table II. The low temperature coefficients of G5, F6 and R10 indicate them to be either solvent shielded or intramolecularly H-bonded.

A large number of inter- and intraresidue nOe's have been observed for the peptide at a mixing time of 300 ms. A survey of all observed nOe's is shown in

Table II. Temperature coefficients of NH chemical shifts and coupling constants ($^3J_{NH\alpha}$, Hz) of Tyr-BK.

Residue	*Amide proton* $-\Delta\delta/\Delta T \times 10^{-3}$ *ppm/K*	$^3J_{NH\alpha}$
Tyr1	–	–
Arg2	–	–
Pro3	–	–
Pro4	–	–
Gly5	2.7	4.4
Phe6	0.6	7.3
Ser7	7.9	5.1
Pro8	–	–
Phe9	5.4	8.8
Arg10	2.1	6.6

figure 3. $d_{\alpha N}$ nOe's were seen from P4 to R10, except for the expected break at P8. d_{NN} nOe's were observed for the central residues G5 to S7 (fig 2c). Two important $d_{\alpha\alpha}$ nOe's were seen, the first between P3 and P4 and the second between S7 and P8 (marked C and D respectively in fig 2b). These nOe's indicate that the amide bond between P3 and P4 and that between S7 and P8 is *cis*. It may be mentioned here that the nOe between P3αH and P4δH (B in fig 2b) fixes the P3–P4 amide bond in the *trans* conformation. This would lead to at least two conformations for Tyr-BK. In the first conformation X, the P3–P4 bond is *trans* with the S7–P8 bond *cis*, while in the second conformation Y, both the P3–P4 and the S7–P8 bonds are *cis*. From the intensity of the nOe's (peaks B and C in fig 2b) it can be inferred that this second conformation Y is a minor conformation. However, the relative populations of the two conformations X and Y are not easy to determine, since NOESY cross-peak intensities depend on mixing time, spin diffusion, exchange processes, etc. The occurrence of both d_{NN} and $d_{\alpha\alpha}$ nOe's shows the presence of a definite secondary structure in the molecule. Based on the available NMR data, ie, temperature coefficients and nOe patterns and our previous work on native BK [3–6], we propose the presence of a first β-turn for the sequence P3–P4–G5–F6 which involves an H-bond between the CO of P3 and NH of F6. The second β-turn occurs at the C-terminal end for the segment S7–P8–F9–R10 and associates the CO of S7 in an H-bond with the NH of R10. This is in agreement with Chou–Fasman calculations which predict a high propensity of β-turns for the above two sequences [22].

In addition to the β-turns discussed above, there may also exist other conformations. This can be inferred from the many weak peaks which appear in the NH region in the 1D-spectrum (fig 1a); however, these conformations could not be easily deciphered.

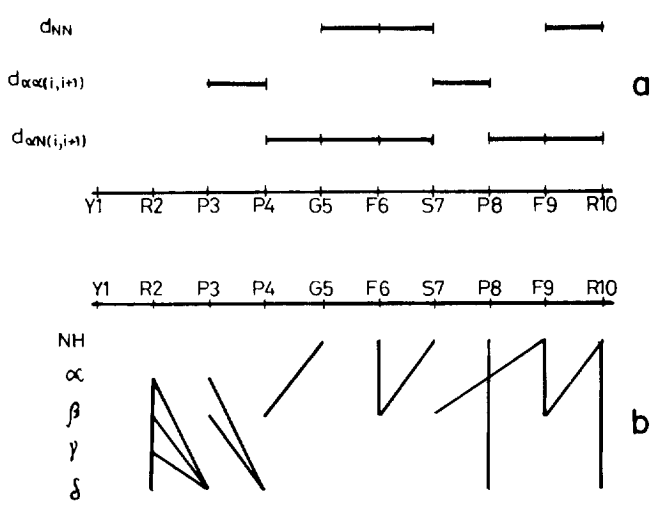

Fig 3. A survey of all observed nOes in Tyr-BK; **a.** nOes along the backbone; **b.** Vertical lines indicate intraresidue nOes, while interresidue nOes are depicted by slanting lines.

Molecular dynamics (MD) simulations

Methodology

Molecular dynamics calculations were performed on a Silicon Graphics Iris Indigo R4000 computer with molecular modeling software from MSI, USA. Computations were carried out with Discover (v 2.9) and the graphic display with Insight II (v 2.3). The energy was calculated with the CFF91 force field [23]. The bond stretching was described by a simple harmonic term. No cross-terms which express the coupling between the internal degrees of freedom were included in the energy expression. A distance-dependent dielectric of $\varepsilon = r$ was used in the Coulombic term. Simulations were carried out only for the dominant conformation (X), for which an unambiguously assigned set of nOe's exists. The S7–P8 omega angle was constrained to *cis*; all other omega angles were fixed as *trans*. A constraining force of 50 kcal mol^{-1} rad^{-2} was applied to all these angles.

All nOe's and H-bonds observed experimentally were used as distance restraints. The nOe's were classified as weak, intermediate and strong; the upper and lower bounds were fixed as 4.2–4.8 Å, 3.4–4.0 Å and 2.8–3.4 Å respectively. The two H-bonds, one between Pro^3 CO and Phe^6 NH and the second between Ser^7 CO and Arg^{10} NH were also cast as distance restraints, with upper and lower bounds of 1.70–2.10 Å for A–H···D (A ≡ acceptor, D ≡ donor) and 2.70–3.10 Å for A···D distances. nOe distances were constrained with force constants of 50 kcal mol^{-1} $Å^{-2}$, while H-bond distances were constrained with 100 kcal mol^{-1} $Å^{-2}$. For methyl groups, β-hydrogens, γ-hydrogens, etc of side chains, a pseudo atom was defined at the centroid of the group and restraint was applied to the pseudo atom. Dynamics were run on the following protocol. The starting structure was energy-minimized with 100 steps of steepest descents to remove any initial strain. The molecule was then 'heated' to 600 K in steps of 100 K, equilibrating for 1.0 ps at each new temperature and resuming dynamics for 1.0 ps. On reaching 600 K, 5.0 ps equilibration was applied, after which dynamics were continued for a further period of 50 ps. Frames from the MD trajectory were stored every 1.0 ps to give 50 structures

which were then subsequently treated. Each of the 50 stored structures was 'cooled' to 300 K with an identical strategy as described for the heating process. Finally, the structures were energy-minimized beginning with 100 steps of steepest descents, followed by 1000 steps of conjugate gradients until the derivative fell below a threshold of 0.001 kcal mol^{-1}. The Newton equations were integrated by a leap-frog scheme with an integration time step of 1 fs (femtosecond). During the equilibration stage the temperature was controlled by direct velocity scaling, while during the data collection period a weak coupling to a temperature bath was adopted.

MD results

For conformation X with only the S7–P8 amide bond constrained as *cis*, the 50 structures generated by MD simulations had an energy spread of 30 kcal/mol. There was no violation of the imposed distance restraints in any of the 50 structures. The maximum RMS deviations of the backbone atoms and side chain of individual amino acids in the 50 structures are given in table III. The arginines (Arg^2 and Arg^9) showed large variations, with RMS deviations of 2.20 and 2.03 Å respectively. In most of the structures the first β-turn around P3–P4–G5–F6 was not strictly definable, but this segment seemed to favor a type II β-turn, while about S7–P8–F9–R10, there was a strong preference for a type I β-turn. In about 28% of the structures, the Gly^5 NH was hydrogen-bonded to Pro^8 CO, and could explain the low temperature coefficient observed for Gly^5 NH (table II). The 50 structures were grouped into families using the global minimum as reference. The classification into families was based on RMS deviations of the backbone atoms. This gave two major families, I and II, with almost an equal number of members for which the range of RMS deviations were 0–1 Å (family I) and 1–2 Å (family II) respectively. A representative structure from each family is shown in figures 4 and 5.

Table III. RMS deviations of backbone atoms and side chains of individual residues in the 50 structures obtained by MD simulations for conformation X.

Atoms	*RMS deviation*
Backbone	2.471
Sidechain	–
Tyr1	0.837
Arg2	2.196
Pro3	0.844
Pro4	0.868
Gly5	–
Phe6	1.786
Ser7	0.582
Pro8	0.757
Phe9	0.737
Arg10	2.031

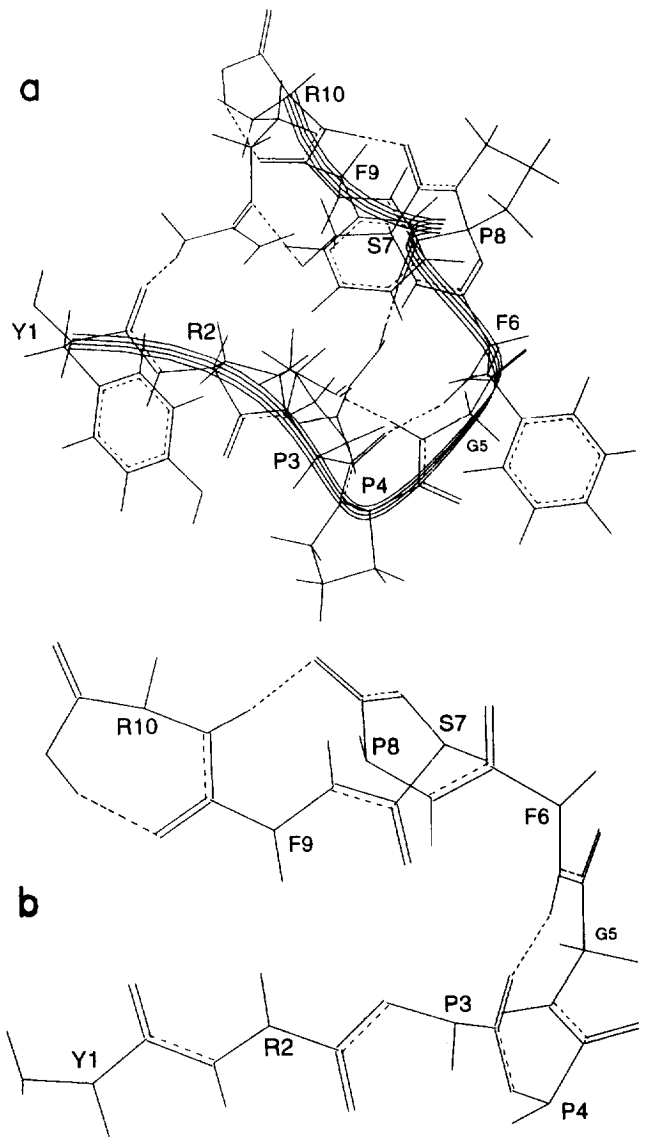

Fig 4. Representative structure of (**a**) family I for conformation X obtained by MD simulations using nOe's as distance restraints. The ribbon traces the backbone atoms. The figure (**b**) alongside is the structure with only backbone atoms shown for clarity.

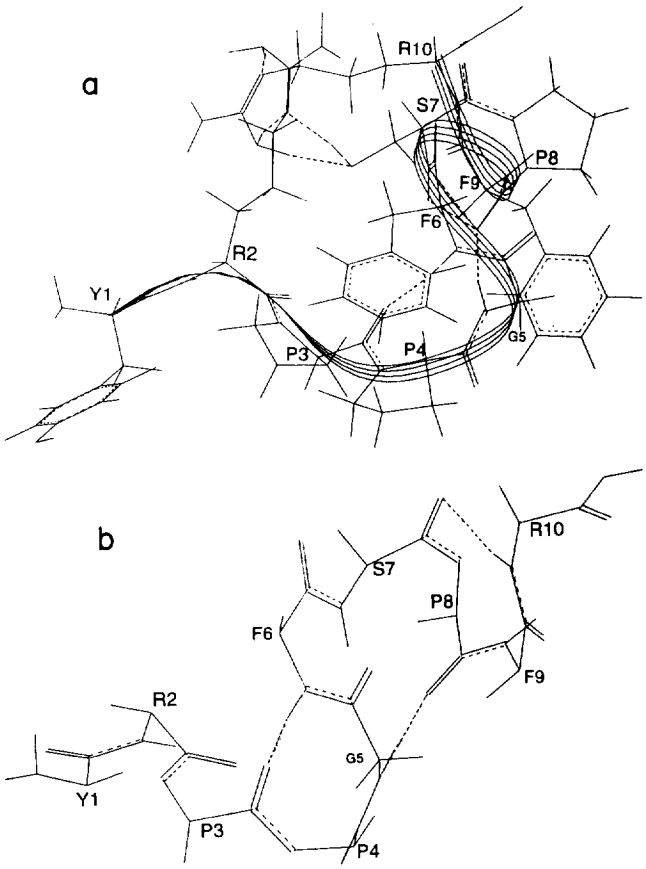

Fig 5. Representative structure of (**a**) family II for conformation X obtained by MD simulations using nOe's as distance restraints. The ribbon traces the backbone atoms. The figure (**b**) alongside is the structure with only backbone atoms shown for clarity.

Conclusions

Using 2D-NMR techniques, Tyr-BK was found to exist in two conformations, X and Y. The most important difference in these two conformations is the *cis/trans* arrangement around the P3–P4 amide bond. Both conformations have the S7–P8 amide bond as *cis*, and β-turns around segments P3–P4–G5–F6 and S7–P8–F9–R10. MD simulations for the major conformation (X) using 20 distance restraints produced a set of structures which had maximum RMS deviations of 2.5 Å in the backbone.

The conformation of native BK was earlier reported by ourselves [6] and shown to have two β-turns around the very same tetrapeptide segments as seen for Tyr-BK. However, in native BK, all amide bonds are *trans*, while in Tyr-BK in both conformations X and Y, the S7–P8 bond is *cis*. This small but crucial difference in the backbone structure possibly explains the slightly lower activity of Tyr-BK.

Acknowledgments

The facilities provided by the National Facility for High-Field NMR located at TIFR and supported by DST, DBT and CSIR are gratefully acknowledged. The Ministry of Human Resource and Development (MHRD) is also thanked for the computational facilities at Bombay College of Pharmacy.

References

1 Regoli D, Barabe J (1980) *Pharmacol Rev* 32, 1–30
2 Goodfriend TL, Ball DLJ (1969) *J Lab Clin Med* 73, 501–506
3 Otter A, Bigler P, Stewart JM, Kotovych G (1993) *Biopolymers* 33, 769–780
4 Sejbal J, Cann JR, Stewart JM, Gera L, Kotovyich G (1996) *J Med Chem* 39, 1281–1292
5 Thurieau C, Félétou M, Hennig P, Raimbaud E, Canet E, Fauchere JL (1996) *J Med Chem* 39, 2095–2101
6 Mirmira SR, Durani S, Srivastava S, Phadke RS (1990) *Magn Reson Chem* 28, 587–593
7 Srivastava S, Haram S, Phadke RS (1991) *Magn Reson Chem* 29, 333–337
8 Srivastava S, Rai SS, Phadke RS (1992) *Phys Med* 8, 137–141
9 Srivastava S, Phadke RS, Govil G (1991) *Proteins: Structure, Dynamics and Design* (Renugopalakishnan V, Carey PR, Smith ICP, Huang SG, Storer AC eds) Escom, Leiden, The Netherlands, 57–61
10 Welsh JH, Zerbe O, Von-Philipsborn W, Robinson JA (1992) *FEBS Lett* 297, 216–220
11 Erdoc EG, ed (1970) *Handbook of Experimental Pharmacology*. Springer-Verlag, New York, 25
12 Nicolaid ED, Dewald HA, Craft MK (1963) *J Med Chem* 6, 739–745
13 Shimamoto K, Ando T, Nakao T, Tanaka S, Sakuma M, Miyhara M (1978) *J Lab Clin Med* 91, 721–728
14 Mashford ML, Roberts ML (1971) *Biochem Pharmacol* 20, 969–973
15 Odya CE, Goodfriend TL, Pena C (1980) *Biochem Pharmacol* 29, 175–185
16 Aue WP, Bartholdi E, Ernst RR (1976) *J Chem Phys* 64, 2229–2246
17 Jeener J, Meier BH, Bachmann P, Ernst RR (1979) *J Chem Phys* 71, 4546–4553
18 Wagner G, Wüthrich K (1982) *J Mol Biol* 155, 347–366
19 Wagner G (1983) *Quart Rev* 16, 1–57
20 Pardi A, Billeter M, Wüthrich K (1984) *J Mol Biol* 180, 741–751
21 Bach AC, Eyermann CY, Gross JD et al (1994) *J Am Chem Soc* 116, 3207–3213
22 Chou PY, Fasman GD (1979) *Biophys J* 26, 367–379
23 Maple L, Dinur U, Hagler AT (1988) *Proc Natl Acad Sci USA* 85, 5350–5355